



## Interstitial Diffusion of Carbon and Nitrogen into Heat-Affected Zones of 11–12% Chromium Steel Welds

*The possibility of introducing austenite stabilizers into the HAZ to restrict grain growth is investigated*

BY A. M. MEYER AND M. du TOIT

**ABSTRACT.** The welding of 11–12% chromium steels is subject to the traditional concern with ferritic grain growth in the heat-affected zone of ferritic stainless steels. The grain growth could be inhibited if austenite on the ferrite grain boundaries could be stabilized at high temperatures.

This article discusses the possibility that diffusion from the weld metal can increase the carbon or nitrogen content of the heat-affected zone, and consequently stabilize grain boundary austenite.

### Introduction

In recent years, considerable interest has developed in the use of 3CR12 by the automotive and agricultural industries (Ref. 1). The cost of additional thickness requirements and surface treatments needed to counteract corrosion loss in conventional carbon steel presents a large portion of the material cost over the life cycle of a component. The interest in 3CR12, therefore, arises from its relative resistance to atmospheric corrosion (Ref. 1). The chemical composition of this corrosion-resistant steel is shown in Table I. However, the traditional concerns regarding grain growth and embrittlement in the heat-affected zones of welds in fer-

ritic stainless steels also apply to 3CR12.

The heat-affected zone in 3CR12 consists of three zones, namely the high-temperature heat-affected zone (HTHAZ), the duplex zone and the low-temperature heat-affected zone (LTHAZ) (Ref. 2). The grain growth that occurs in the HTHAZ during welding is the main cause of concern. The phase composition of the heat-affected zone at high temperatures depends on the relative amount of austenite and ferrite stabilizers in the steel (Ref. 3). During cooling, grain growth is restricted by grain boundary austenite (Ref. 3). Considerable ferrite grain growth occurs during the heating cycle and close to the peak temperature when the phase composition is fully ferritic (Ref. 3).

The research done for this article explores the possibility of introducing austenite stabilizers into the heat-affected zone during welding to restrict

grain growth through forming a dual-phase ferritic-austenitic structure close to the peak temperature reached during welding. The width of the heat-affected zone is a function of the heat input during welding (Ref. 4).

### The Influence of Ferrite Grain Size on Impact Properties

Ferrite grain size has a marked effect on the impact properties of the HTHAZ. Ductile-to-brittle-transition-temperature (DBTT) results from samples obtained through temperature-cycle simulation by Gooch and Ginn (Ref. 5) indicate the DBTT of 12% ferritic-martensitic steel increases with the ferrite grain size.

The Petch relationship between transition temperature and grain size is given by the form (Ref. 5)

$$DBTT = F + G \ln(d^2) \quad (1)$$

where F and G are constants and d is the grain diameter.

The DBTT results obtained by Gooch and Ginn (Ref. 5) are plotted against  $\ln(d^2)$  in Fig. 1. An approximate correlation with Equation 1 was found. This indicates the ferrite grain size would play a major role in the fracture toughness of the HTHAZ in 3CR12 welds.

### The Influence of Martensite

It is well established that grain growth may only account for part of the observed

### KEY WORDS

Austenite  
Ferrite  
HAZ  
Ferritic Stainless  
Grain Growth  
Embrittlement

A. M. MEYER is with Metpro, a Division of Dornyl, Pretoria, South Africa. M. du TOIT is with the Dept. of Materials Science and Metallurgical Engineering, University of Pretoria, South Africa.





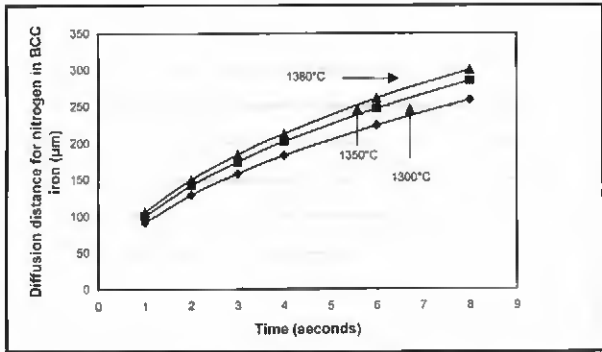


Fig. 7 — Calculated diffusion distances for nitrogen in BCC iron.

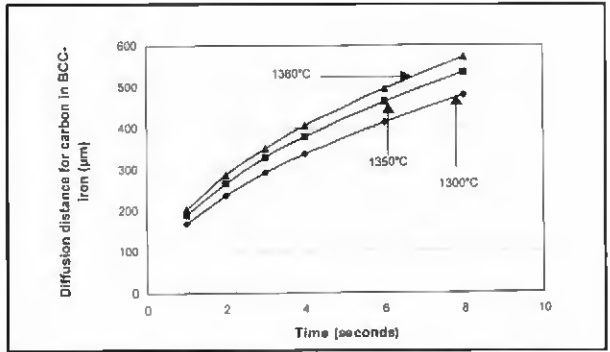


Fig. 8 — Calculated diffusion distances for carbon in BCC iron.

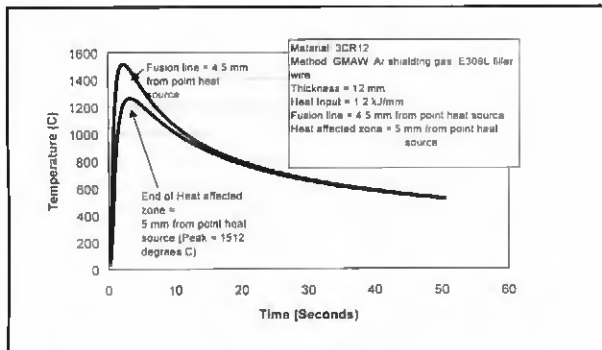


Fig. 9 — Temperature sequence prediction from the Rosenthal equation (Ref. 4).

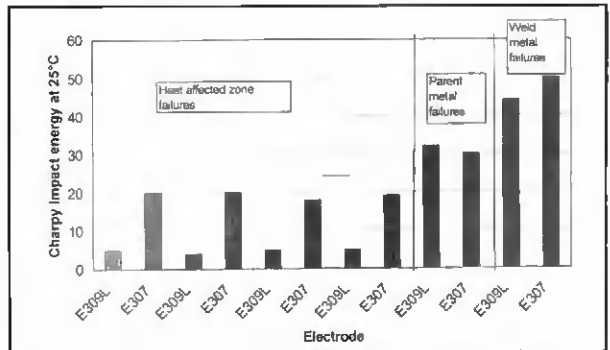


Fig. 10 — Charpy impact energy values at 25°C (SMAW, heat input = 0.7 kJ/mm).

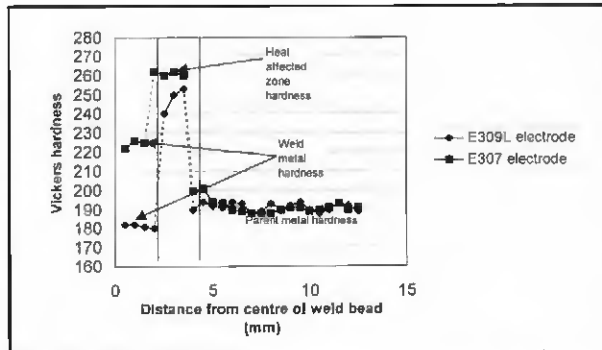


Fig. 11 — Hardness profile for welds in 8-mm 3CR12 (SMAW, heat input = 0.7 kJ/mm).

ritscope™ readings) were 15.5 FN in the weld metal of the E309L electrode and 13.1 FN in the same region of the E307 weld metal. Usually, a ferrite number of at least five is required in austenitic weld metals to prevent hot cracking during cooling.

All metallographic samples were prepared by polishing to a finish of 1 µm. Etching was done by quick swabbing with Kalling's No. 2 etching reagent.

The heat-affected zone hardness of the E307 weld is higher than the hardness in the same region of the E309L welds. This corresponds to the observed smaller grain size and larger fraction of grain

boundary martensite. The absorbed Charpy impact energy is also higher for the heat-affected zone in the E307 welds than for the E309L welds, as can be seen in Fig. 10. The higher hardness, together with improved impact energy, may render the protection of the heat-affected zone by plastic deformation of the softer base metal and weld metal to be more likely (Ref. 2). This mechanism should increase the overall integrity of the weld in impact situations.

Half-size Charpy impact specimens (5 x 10 x 55 mm) were machined from each of the E309L and E307 welds. The specimens were cut across the weld beam, with the notch tip perpendicular to the rolling direction and the plate thickness on the 5-mm side. The notch tip was carefully directed into the high-temperature heat-affected zone with the notch tip parallel to the welding direction. Weld metal failures (crack located in the weld metal), base metal failures (crack located in the base metal), and heat-affected zone failures

(crack located in the heat-affected zone) were observed, due to the fact that accurate placing of the crack tip in the heat-affected zone is not always possible. In the heat-affected zone failures of the E307 welds, the crack appeared to swerve away from the harder heat-affected zone into the base metal, resulting in higher absorbed Charpy impact energy values. Hardness profiles across the two different welds are shown in Fig. 11. The higher hardness of the 307 weld metal was expected due to the higher carbon content of the E307 electrode (0.16%) compared to that of the E309L electrode (<0.03%).

**Gas Metal Arc Welding**

Experimental gas metal arc welding (GMAW) was done on 12-mm hot-rolled 3CR12 plate. The heat input was held constant at 1.3 kJ/mm. Three separate welds were made using the following:

- 1) ER309L filler metal containing 0.03% carbon (1.2 mm) and pure argon shielding gas. The microstructure of the heat-affected zone is shown in Fig. 12.
- 2) ER307 filler metal containing 0.16% carbon and a pure argon shielding gas. The microstructure of the heat-affected zone is shown in Fig. 13.
- 3) ER309L filler metal containing

0.03% carbon (1.2 mm) and an argon +33% nitrogen shielding gas mixture. The microstructure of the heat-affected zone is shown in Fig. 14.

The weld metal microstructure of each of the welds consisted of austenite and ferrite. The average Fischer Ferritoscope readings were 15.1 FN for the ER309L welds with pure argon shielding gas, 12.8 FN for the ER307 welds with pure argon shielding gas and 5.9 FN for the ER309L welds with the Ar-N<sub>2</sub> mixture. The low ferrite number of the weld with the Ar-N<sub>2</sub> mixture suggests that the nitrogen level in the ER309L weld metal was raised and that the austenite was stabilized by the higher nitrogen content. Although the ferrite number is still more than five, the susceptibility of the weld metal to hot cracking may be increased by the lower ferrite content.

The grain sizes in the heat-affected zones of the different welds were determined in a similar fashion as described earlier with the shielded metal arc welds. The average ASTM grain size number in the heat-affected zone of the ER309L weld with pure argon shielding gas was 1-2, while in the heat-affected zones of the ER309L welds with the Ar-N<sub>2</sub> shielding gas mixture and the ER307 welds with pure argon shielding gas, the average ASTM grain size number was 4-5. Therefore, a smaller ferrite grain size was observed in the heat-affected zones of the ER309L welds with the Ar-N<sub>2</sub> shielding gas mixture and the ER307 welds with pure argon shielding gas than in the heat-affected zone of the ER309L weld with pure argon shielding gas. In the heat-affected zones of the ER309L weld with the Ar-N<sub>2</sub> mixture and the ER307 weld, a larger fraction of grain boundary martensite was also observed. In accordance with these observations, the heat-affected zones of these two welds were harder than the heat-affected zone of the ER309L weld with pure argon shielding gas. Hardness profiles across these welds are shown in Fig. 15. Contrary to expectation, the ER307 weld metal hardness is only marginally higher than that of the ER309L. This may be due to the fact higher peak temperatures are reached in GMAW as compared with SMAW, and, consequently, the interstitial elements could diffuse out of the weld metal faster than during SMAW.

The smaller grain size in the heat-affected zones of the ER309L weld with the Ar-N<sub>2</sub> mixture and the ER307 weld with the pure Ar shielding gas, together with the higher hardness, would render the protection of the zone by the softer weld metal and base metal to be more likely in impact situations (Ref. 2), and would increase the overall integrity of the

weld. Similar to the SMAW specimens discussed previously, three types of failures were observed in the full-size Charpy specimens (10 x 10 x 55 mm) machined from the welds. The notch was placed perpendicular to the rolling direction and the plate thickness. Proper Charpy specimens could not be obtained from the Ar-N<sub>2</sub> welds because of the excessive spatter that occurred in these welds. The spatter is similar to that observed when shielding gas flow is insufficient to prevent air contamination of the shielding gas, and may therefore be directly attributed to the nitrogen present in the shielding gas. As a result, only the ER309L and ER307 welds (both with pure argon shielding gas) were evaluated. The results are shown in Fig. 16. Higher impact energies are observed in Fig. 16 than in Fig. 10, due to the fact full-size Charpy specimens were used instead of the half-size specimens used with the shielded metal arc welds.

#### Chemical Analysis

Chemical analysis of the base metal, weld metal, and heat-affected zone was done to confirm the transfer of carbon and nitrogen across the weld interface. The heat-affected zone samples were obtained from very fine drillings (0.5-mm-diameter drill) from lightly etched specimens. Etching was done by quick swabbing with Kalling's nr. 2. The results are tabulated in Table 4.

The high levels of carbon (HTHAZ of ER307 + Ar) and nitrogen (ER309L + Ar-N<sub>2</sub>) suggest that interstitial diffusion of carbon and nitrogen may have taken place. Contamination of the heat-affected zone samples from either the weld metal or the base metal was inescapable but care was taken to take the drilling as far as possible from the weld metal to get contamination from a region with a lower interstitial content rather than from the weld metal with the higher carbon and nitrogen content. The results nevertheless show an increase of 96% in carbon content and 78% in nitrogen content. The large increase in interstitial content suggests that contamination of the sample drillings of the heat-affected zone

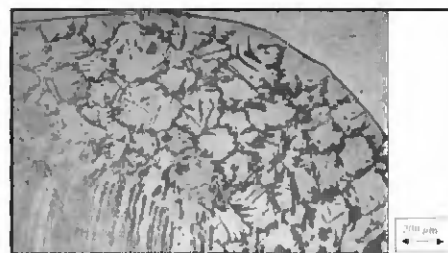


Fig. 12 — The microstructure of the heat-affected zone in 3CR12 (GMAW, 1.3 kJ/mm, ER309L filler metal, argon shielding, 100X).

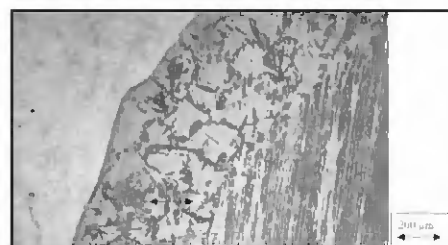


Fig. 13 — The microstructure of the heat-affected zone in 3CR12 (GMAW, 1.3 kJ/mm, ER307 filler metal, argon shielding, 100X).

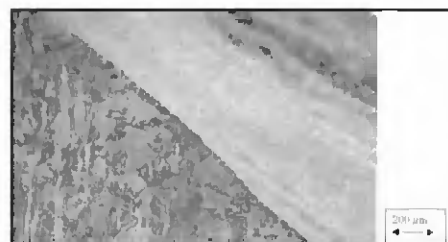


Fig. 14 — The microstructure of the heat-affected zone in 3CR12 (GMAW, 1.3 kJ/mm, ER309L filler metal, argon-nitrogen shielding, 100X).

by the weld metal may have influenced the result of the chemical analysis.

#### Continuous Cooling and Diffusion

It was mentioned earlier that the isothermal conditions assumed in the diffusion distance calculations were not valid, since the welded plate cools continuously. In order to get a more acceptable model of the interstitial diffusion of car-

Table 4 — Carbon and Nitrogen Contents in Different Zones of Welds in 3CR12

Process (welding wire and shielding gas)	Base Metal		Heat-Affected Zone		Weld Metal	
	%C	%N	%C	%N	%C	%N
ER309L + Ar	0.029	0.019	0.031	0.018	0.032	0.024
ER309L + Ar-N <sub>2</sub>	0.033	0.018	0.028	<b>0.050</b>	0.032	0.092
ER307 + Ar	0.027	0.017	<b>0.053</b>	0.019	0.130	0.020

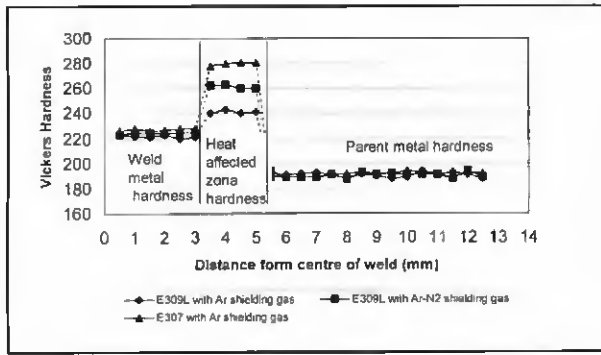


Fig. 15—Hardness profile for welds in 12-mm 3CR12 (GMAW, heat input = 1.3 kJ/mm).

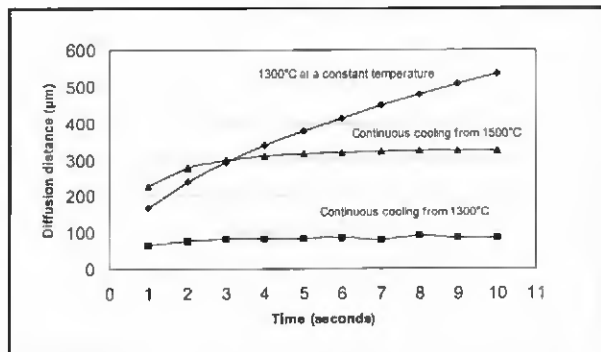


Fig. 17—Diffusion distance calculated for carbon in 3CR12 for a constant temperature of 1300°C and continuous cooling from 1300°C and 1500°C.

hon during the cooling period of a weld, a temperature sequence for the weld interface (1500°C) of a 1.0 kJ/mm weld in 12-mm 3CR12 plate was constructed from the Rosenthal equation (Ref. 4). In order to construct the sequence, a period of 40 s was divided into time intervals of 0.1 s. The diffusion coefficient was calculated at the end of each interval, using the temperature at that time. The average diffusion coefficient was then determined after 1-s intervals up to 10 s.

The results of these calculations are shown in Fig. 17, together with the earlier results when isothermal conditions were assumed. The continuous cooling has a definite decreasing effect on the theoretical diffusion distance. The results as discussed earlier predict a diffusion distance of 479  $\mu\text{m}$  after 8 s and 535  $\mu\text{m}$  after 10 s, at a constant temperature of 1300°C. On the other hand, continuous cooling from 1300°C only predicts a diffusion distance of 85  $\mu\text{m}$  after 10 s.

If the weld interface is assumed to form at 1500°C (the approximate melting point of 3CR12), and continuous cooling as predicted by the Rosenthal equation (Ref. 4) is taken into account, the theoretical diffusion distance is 326  $\mu\text{m}$  after 10 s. The

microstructural changes and the difference in impact properties as observed in the experimental welds discussed earlier therefore seems to be the result of interstitial diffusion from the weld metal into the base plate across the weld interface. Ferrite grain growth in the heat-affected zones of welds in 3CR12 has a detrimental effect on the impact properties of the welded joint. Ferrite grain growth can be inhibited by increasing the amount of grain boundary austenite in the heat-affected zone at high temperatures. Increasing carbon or nitrogen contents in the heat-affected zone should act to stabilize grain boundary austenite. Consequently, a decrease in ferrite grain growth should be observed in the heat-affected zone of 3CR12 welds.

A decrease in the ferrite grain size occurs in the heat-affected zones of welds in 3CR12 if the carbon or nitrogen content of the weld metal is increased. The finer heat-affected zone structure improves the impact properties of the welded joint. Diffusion distance calculations suggest that the finer structure, increase in grain boundary austenite, and improvement in impact properties are the result of diffusion of carbon and nitrogen from the weld metal, across the weld interface and into the heat-affected zone. Although an increase in the interstitial content of the heat-affected zone was observed in chemical analysis, contamination of the heat-affected zone samples by the weld metal could not be ruled out. Therefore, the chemical analysis should not be viewed as conclusive. A filler metal with a different interstitial content, however, may conclu-

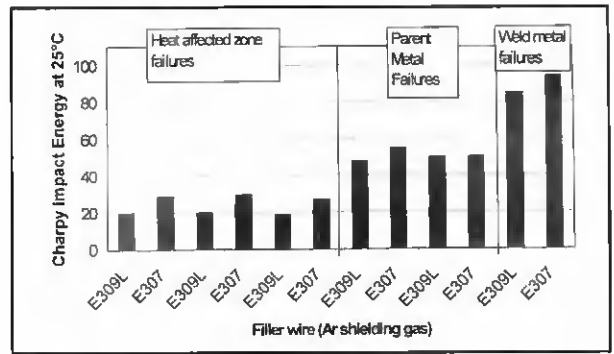


Fig. 16—Charpy impact values at 25°C (GMAW, heat input = 1.3 kJ/mm).

sively alter the phase composition of the heat-affected zone.

#### References

1. *Product Guide for 3CR12*. 1988. Middelburg Steel and Alloys (Pty) Limited, (1): 14-19.
2. Grobler, C. 1987. Weldability studies on 12% and 14% chromium steels. Ph.D., pp. 62-79 and 86-122.
3. Zaayman, J. J. J. 1992. The heat-affected zone toughness of welds in 11 to 12 per cent chromium steels. *M. Eng.* (UP), pp. 31-71 and 76-93.
4. Easterling, K. 1993. *Introduction to the Physical Metallurgy of Welding*. Butterworth, Heinemann; Oxford, Second Edition 1992, Second Impression 1993, pp. 1-38.
5. Gooch, T. G., and Ginn, B. J. 1988. Heat-affected zone toughness of MMA welded 12%Cr martensitic-ferritic steels. Report from the cooperative research program for research members only. The Welding Institute, Cambridge, England, pp. 3-30.6.
6. Hawkins, D. N., Beech, J., and Valtierra-Gallardo, S. 1988. A new approach to microstructural control in duplex stainless steel welds. Sheffield, pp. 199-203.
7. Guy, A. G. 1972. *Introduction to Materials Science*. New York, N.Y.: McGraw-Hill Book Co.